General Disclaimer

One or more of the Following Statements may affect this Document

- This document has been reproduced from the best copy furnished by the organizational source. It is being released in the interest of making available as much information as possible.

- This document may contain data, which exceeds the sheet parameters. It was furnished in this condition by the organizational source and is the best copy available.

- This document may contain tone-on-tone or color graphs, charts and/or pictures, which have been reproduced in black and white.

- This document is paginated as submitted by the original source.

- Portions of this document are not fully legible due to the historical nature of some of the material. However, it is the best reproduction available from the original submission.

JPL PUBLICATION 83-5

Linear Retrieval and Global Measurements of Wind Speed from the Seasat SMMR

Prem Chand Pandey

March 1, 1983

National Aeronautics and
Space Administration

Jet Propulsion Laboratory
California Institute of Technology
Pasadena, California

JPL PUBLICATION 83-5

Linear Retrieval and Global Measurements of Wind Speed from the Seasat SMMR

Prem Chand Pandey

March 1, 1983

NASA
National Aeronautics and
Space Administration

Jet Propulsion Laboratory
California Institute of Technology
Pasadena, California

The research described in this publication was carried out by the Jet Propulsion Laboratory, California Institute of Technology, and was sponsored jointly by the National Academy of Sciences and the National Aeronautics and Space Administration.

Contents

Tables

Contents (Contd.)

Figures

Abstract

Retrievals of wind speed (WS) from Seasat Scanning Multichannel Microwave Radiometer (SMMR) have been performed using a two-step statistical technique. Nine subsets of two to five SMMR channels were examined for wind speed retrieval. These subsets were derived by using a leaps and bounds procedure based on the R^2 coefficient of determination selection criteria to a statistical data base of brightness temperatures and geophysical parameters. Analysis of Monsoon Experiment (MONEX'79) and ocean station PAPA (50°N, 145°W) data showed a strong correlation (correlation coefficient ~.77) between sea surface temperature and water vapor. This relation was used in generating the statistical data base. A comparison of SMMR-WS with Joint Air-Sea Interaction Experiment (JASIN) surface wind speed shows an rms accuracy of ~1.5 m/sec for a wind speed range of 3-16 m/sec. The retrieval accuracy of WS from different subsets agreed to within about 10 percent.

Global maps of WS have been produced for one and three month periods. These maps show the global distribution of winds in well organized belts. The tropical easterlies are found to be of comparable strength in both hemispheres whereas westerlies of the southern hemisphere are stronger than those of the northern hemisphere. These maps reveal the previously known features and conform to the prevailing ideas. A comparison of global maps of wind speed from SMMR, Seasat-A Scatterometer (SASS) and Altimeter (ALT) shows some similarities and discrepancies which need further investigation.

1. Introduction

The Scanning Multichannel Microwave Radiometer (SMMR) aboard Seasat and Nimbus-7 satellites was intended to monitor global sea surface temperature, wind speed, water vapor, liquid water content and rain fall rate over oceanic regions. The SMMR measured microwave radiation at 6.6, 10.69, 18.0, 21.0 and 37.0 GHz and in both horizontal and vertical polarizations from which surface and atmospheric parameters are inferred. A recent review article by Njoku [1982] describes the passive microwave remote sensing of the ocean and atmospheric parameters from space-borne radiometers.

Recently we (Pandey and Kakar, 1983) have developed a linear two-step statistical technique to retrieve geophysical parameters from microwave radio metric data. The technique has already been used to retrieve sea surface temperature [Pandey and Kniffen, 1982] and precipitable water [Pandey, 1982] from Seasat SMMR data.

The purpose of this document is to retrieve ocean surface wind speed from SMMR measurements using the previously developed statistical technique of the authors and compare the SMMR retrieved wind speed with in situ observation during Joint Air-Sea Interaction (JASIN) experiment. Comparison with Chester's [Lipes and Born, 1981] geophysical algorithm which has been used at Jet Propulsion Laboratory for processing Seasat SMMR data will also be made.

Seasat also carried a scatterometer called Seasat-A Satellite Scatterometer (SASS) and an altimeter (ALT) for measuring wind speed. SASS also measured wind direction. An intercomparison of wind speed derived from both active and passive sensors aboard Seasat will provide confidence to users of the data about the quality of the retrieved parameter. At present there are only a few thousand (~2000) widely scattered ship reports per day and even fewer data buoy measurements of wind speed over the vast oceanic regions. Seasat provided

several thousands wind vectors per day which have been used in a numerical experiment at Goddard Laboratory for Atmospheric Sciences [Gower, 1981] to test the utility of Seasat wind vector in improving weather forecasting. These experiments have shown a strong impact of Seasat data in improving short range forecasts (2-3 day). The Indian monsoon is one of the most important wind patterns in the world. The ability to measure winds over the Indian ocean (including the Arabian sea extending up to Somali coast, and the Bay of Bengal) and to calculate the ocean circulation will greatly enhance our understanding of the monsoon. Calculations of the momentum, heat and water vapor fluxes across the ocean-atmosphere system also require an accurate knowledge of surface wind speed. More confidence in synoptic weather analysis is gained when wind field is available as an additional input. All these studies demonstrate the usefulness of wind measurements for meteorological and oceanographic purposes. National Oceanic Satellite System (NOSS) or any other similar system if implemented will provide these data in real time and perhaps with better capability.

2. Seasat Scatterometer and altimeter

The Seasat SMMR instruments have been described in detail by Njoku et al. (1980). A brief description and characteristics of scatterometer and altimeter relevant to the intercomparison and interpretation of data will be given here. For more detail, the reader is referred to several articles published in Journal of Geophysical Research, Seasat special issue, [Bernstein, 1982].

The Seasat-A Satellite Scatterometer (SASS) operated at 14.6 GHz and was used to measure wind vector over oceans with an accuracy of ±2 m/sec or 10% (whichever is greater) over a range of 4-26 m/sec and wind direction 0 to 360 deg with an accuracy of ± 20 deg. The instrument used four dual-polarized

antennas, each oriented 45 deg relative to the subsatellite track, and provided measurements of normalized radar cross section (NRCS) σ^o. The σ^o, is a function of wind speed. The wind field produces capillary waves which modify the radar backscatter through the process of Bragg scattering. The scatterometer has three separate swaths, one centered on at nadir and the other two on the right and left side of the subsatellite track. The nadir swath is ±7[illegible] km and off nadir swaths begin at about 200 km cross track from nadir and extend to about 700 km from nadir. The resolution cell is ~50 km.

The altimeter, which operated at 13.5 GHz, has a swath of 2.4 - 12 km centered at nadir depending on the sea state. The instrument was primarily intended to measure satellite altitude, significant wave height and wind speed.

The SMMR swath was ~600 km. For grid 2, the SMMR swath is divided into seven columns ~86 km wide, the resolution of SMMR 10.7 GHz channel. The SMMR processed data is available at 4 different grid sizes. We have used grid 2 data for wind speed retrieval. The 600 km swath starts ~50 km on the left side of the subsatellite track and extends to 550 km on the right side of the track.

3. Radiative transfer equation

For the nonscattering atmosphere in local thermodynamic equilibrium, which is the case for gaseous absorption at microwave frequencies, the radiative transfer equation is given by

$$T_B(\nu) = T_u(\nu) + \tau_\nu(o,h)[\varepsilon(\nu)\, T_s + (1-\varepsilon(\nu))\, T_d(\nu) + (1-\varepsilon(\nu))\, \tau_\nu(\infty,o)\, T_c] \quad (1)$$

$$T_u(\nu) = \int_o^h T(z)\, \frac{\partial \tau_\nu\,(z,h)}{\partial z}\, dz \quad (2)$$

$$T_d(\nu) = \int_{\infty}^{0} T(z) \frac{\partial \tau_\nu(o,z)}{\partial z} \, dz \qquad (3)$$

$$\tau_\nu(z_1,z_2) = \exp\left[-\int_{z_1}^{z_2} \alpha_\nu(z) \, dz\right] \qquad (4)$$

where T_u and T_d are, respectively, the upward and the downward radiating brightness temperature contributions due to the atmosphere, T_s is the surface temperature, T_c is the cosmic background brightness temperature and ε is the surface emissivity. The upward and the downward brightness temperature components are integrals of the atmospheric temperature profile T(z) weighted by the vertical derivative of the transmittance function $\tau_\nu(z_1,z_2)$. The limits of integration are from the surface to satellite altitude h. The transmission function is expressed in terms of α_ν, the atmospheric absorption coefficient due to water vapor, oxygen and liquid water. Equation (1) assumes an approximately specular reflection at the ocean surface. The equation was computed by dividing the atmosphere into concentric layers, each with a specified temperature and absorption coefficient, and using a summation to approximate the integrals. Cloud layers can be inserted at any altitude by modifying the absorption coefficients to include an appropriate amount of liquid water. In addition, the relative humidity of air was assumed to be 100% in the presence of clouds.

4. Retrieval algorithm

Retrieval techniques described in the literature include, among others, statistical [Waters et al., 1975, Grody, 1976, Wilheit and Chang, 1980, Hofer and Njoku, 1981, Pandey and Kakar, 1983], non-linear iterative [Wentz, 1982], and fourier transform techniques, the latter developed by Rosenkranz (1978). The retrieval equations discussed and used here have been derived using a

two-step statistical technique described in detail by Pandey and Kakar (1983). The technique is based upon the application of an efficient algorithm, known as 'regressions by leaps and bounds' [Furnival and Wilson, 1974], to a statistical data base in order to select the 'best' subsets of radiometric channels. The 'best' is defined using the R^2 coefficient of determination criterion, widely used in statistical literature. Our approach is unique in the sense that it provides an opportunity to examine a number of subsets and also different subsets of the same size, which is not possible by other methods. The statistical data base consists of an ensemble of realistic sea surface temperatures, wind speeds, atmospheric water vapor profiles, temperature profiles and cloud models and is summarized in an earlier paper [Pandey and Kakar, 1983]. Our approach of generating a data base is also different than that used by earlier investigators. We have used a second degree polynomial equation between water vapor and SST which exists in nature to generate the data base, along with other parameters. Water vapor versus sea surface temperature curve showed a large scatter with a standard deviation of ~.65 g/cm^2. This relation was obtained from the analysis of data obtained from ocean station PAPA (50°N, 145°W) and Monex '79 experiment. The correlation analysis gave a value of 0.77 for the coefficient of correlation. These are used to calculate brightness temperatures by means of a surface emission model [Pandey and Kakar, 1982] and a radiative transfer model as described in section 3. The retrieval equations are then obtained by using multiple linear regression on the selected subsets, based upon the statistical relationship between geophysical parameters and the calculated brightness temperatures. Non-linearity of the regression parameters was mitigated by using functions of brightness temperature [$f(T_B) = \ln (280-T_B)$] for high frequency (18.0, 21.0, 37.0 GHz) channels. Theoretical brightness temperatures were perturbed by Gaussian noise, characteristic of the SMMR instruments, which smoothed

the regression coefficients and provided a more realistic approach to the problem.

The results of the leaps and bounds algorithm for selecting the best subsets of 2 to 5 channels for retrieving WS are given in Table 1 along with R^2 coefficient of determination values. Four other best subsets of each size are also given in the same Table and may be used for analysis as well. This capability could be exploited to set up a quality control criterion in future algorithms as proposed in the earlier paper [Pandey & Kakar, 1983]. Selection of the best subsets has been made from all of the 10 SMMR channels. We have dropped those subsets which selected 6.6 GHz frequencies, since we are primarily interested in retrieving WS over a grid size of 86 x 86 km and only 10.69, 18.0, 21.0 and 37.0 GHz data has been processed on this grid size. Table 2 gives the regression coefficients for the different subsets using 2 to 5 channels. The coefficients in Table 2 are related to brightness temperature or its function as defined earlier through the following parameter retrieval equation:

$$p = \sum_j a_j T_B{}^j + a_0 \quad , \tag{5}$$

where the $T_B{}^j$'s are functions of the brightness temperature for 18.0, 21.0 and 37.0 GHz or the brightness temperature for 10.69 GHz channel frequencies and a_0 is the intercept. The index j refers to the number of channels. The rms error is also shown in the Table, which decreases as the number of channels increases from 2 to 5. These rms errors are dependent upon the range of variations of the geophysical parameters used in the statistical data base.

5. Bias determination using Chester's algorithm and Seasat-A Scatterometer (SASS) data

Chester's algorithm is being used at Jet Propulsion Laboratory for

Table 1. Results of the leaps and bounds technique in selecting the best subsets of two to five SMMR channels for wind speed determination. Four other subsets of each size are also given as an example.

Size of the subset	Criterion R^2	Variables selected
2	95.29	10.6H, 18.0V
	90.80	10.6H, 18.0H
	84.24	10.6H, 10.6V
	84.08	10.6H, 21.0V
	83.73	10.6H, 37.0H
3	96.37	10.6H, 10.6V, 18.0V
	96.35	10.6H, 18.0V, 18.0H
	96.10	10.6H, 18.0V, 21.0H
	96.08	6.6V, 10.6H, 10.0V
	95.91	6.6H, 10.6H, 18.0V
4	97.62	10.6H, 10.6V, 18.0V, 21.0H
	97.61	10.6H, 10.6V, 18.0V, 37.0H
	97.60	6.6H, 10.6H, 18.0V, 37.0H
	97.60	10.6V, 10.6H, 18.0V, 21.0V
	97.52	6.6V, 10.6H, 18.0V, 37.0H
5	98.73	6.6V, 10.6H, 18.0V, 21.0H, 37.0H
	98.72	10.6V, 10.6H, 18.0V, 21.0H, 37.0H
	98.71	6.6V, 10.6H, 18.0V, 21.0V, 37.0H
	98.69	10.6V, 10.6H, 18.0V, 21.0V, 37.0H
	98.44	10.6V, 10.6H, 18.0V, 21.0H, 37.0V

Table 2. Regression coefficients of some of the subsets given in Table 1. Coefficients are obtained from 600 statistical data base. $F(T_B) = \ln (280. - T_B(\nu))$ is used for 18.0, 21.0 and 37.0 GHz channels.

		Regression coefficients for SMMR channels (GHz)								
Subset size	Intercept	10.6 V	10.6 H	18.0 V	18.0 H	21.0 V	21.0 H	37.0 V	37.0 H	RMS error (m/sec)
2	-356.1579	-	1.3049	51.8733	-	-	-	-	-	1.73
	-416.1711	-	1.4076	-	57.1925	-	-	-	-	2.42
3	-271.3673	-0.3710	1.4061	44.0337	-	-	-	-	-	1.52
	-396.2056	-	1.3587	64.4522	-	-	-5.8645	-	-	1.57
	-274.6716	-	1.1397	89.5278	-47.3220	-	-	-	-	1.52
4	-227.1326	-0.6195	1.5023	44.7312	-	-	-7.0400	-	3.2806	0.90
	-296.4880	-0.5302	1.5379	58.5506	-	-6.9191	-	-	-	1.23
	-191.5762	-0.5549	1.4179	29.1408	-	-	-	-	3.4881	1.23
	-304.0932	-0.4512	1.4965	59.6531	-	-	-7.4781	-	-	1.23
5	-227.1326	-0.6195	1.5023	44.73112	-	-	-7.0400	-	3.2806	0.90

geophysical processing. This algorithm, which essentially is a tuned version of Wilheit and Chang's algorithm, has undergone several tests and evaluation during various workshops [Bussinger et al., 1980, Alishouse, 1982]. As such it was decided to determine the bias of different subsets for wind speed retrieval using Chester's algorithm so that more surface data (in situ measurements) are available for independent verification of the algorithm.

Two-hundred data points from ascending Seasat revolutions over the Pacific ocean between latitude +50°N to-50°S were obtained. These data covered the period from Sept. 16 to Sept. 21, 1978 and provided retrieved wind speed using Chester's algorithm in the range of 3 m/sec to 10 m/sec. Wind speed calculated from different subsets using the present algorithm and its comparison with wind speed from Chester's algorithm are given in Table 3. An examination of Table 3 shows that a large bias results between different subsets and the accuracy of different subsets varies from 0.96 m/sec for a four-channel subset to 1.55 m/sec for a two-channel subset. The large bias in wind speed measurements appears to have its origin in the use of inadequate surface and atmospheric models used in the radiative transfer calculation and/or calibration of the SMMR instruments.

Wind speed from SASS revolution 1120 (VV polarization) and from the matching SMMR cells on grid 2 was also used to estimate the bias. An average of wind speed obtained from SASS which provided four solutions was used for comparison. The bias applied to our algorithm is the average of the bias obtained in Table 3.

6.0 Wind speed comparisons with JASIN surface measurements

6.1 Surface observations

JASIN was planned by British and American scientists as a contribution to

Table 3. Determination of bias from comparison with Chester's algorithm and SASS measurements of WS from Rev 1120

Channels of subset	Bias with Chester's algorithm m/sec	Bias with SASS wind m/sec	RMS difference with Chester's algorithm m/sec
10H, 18V	-4.13	-4.01	1.24
10H, 18H	-8.37	-8.10	1.55
10V, 10H, 18V	1.41	1.30	1.14
10V, 18V, 21H	-8.27	-7.25	1.40
10V, 18V, 18H	-0.73	-0.48	1.14
10V, 10H, 18V, 21V	-2.85	-2.95	0.96
10V, 10H, 18V, 37V	-3.71	-4.13	0.97
10V, 10H, 18V, 21H	3.06	3.17	1.18
10V, 10H, 18V, 21H, 37H	-2.80	-2.95	1.14

the Global Atmospheric Research Program (GARP) and fortunately it coincided with the mission life of Seasat satellite and provided an excellent source of comparison data for geophysical algorithm validation. It has been described in detail in a Seasat-JASIN workshop report [Businger et al., 1980]. A brief description of the aspects of JASIN relevant to the present investigation is given below.

Figure 1 shows the regions in the JASIN experimental area which involved 14 ships, 3 aircraft and 35 mooring systems and took place in deep water off northwest Scotland during July to September 1978. The data on the meteorological ships were recorded both manually at hourly intervals (WMO format) and automatically at one minute intervals.

The wind speed measurements used for the present study consist of a set of data taken by a Gill anemometer on F.S. Meteor during JASIN experiment. They are described by Liu and Large [1981]. The Meteor was stationed at 59°N, 12.5°W, in the north Atlantic about 400 km northwest of Scotland.

The WMO reports provided wind speed measurements by a cup anemometer. In addition, dry and wet bulb temperatures were obtained by Assman psychrometer at 11 m height, and sea surface temperature by bucket method. The accuracies of these data sources have been accessed in the Seasat-JASIN Workshop Report [Businger et al., 1980] to be ± 1 m/sec, on a 20 minute average basis.

6.2 Conversion of recorded wind speed to 19.5 m neutral stability wind speed

The wind speed data were available at different measurement heights. These wind speeds were adjusted to 19.5 m height above the sea surface. A surface-layer parameterization model developed by Liu et al. [1979] at Jet Propulsion Laboratory was used to make this conversion. The model utilized measurements of sea surface

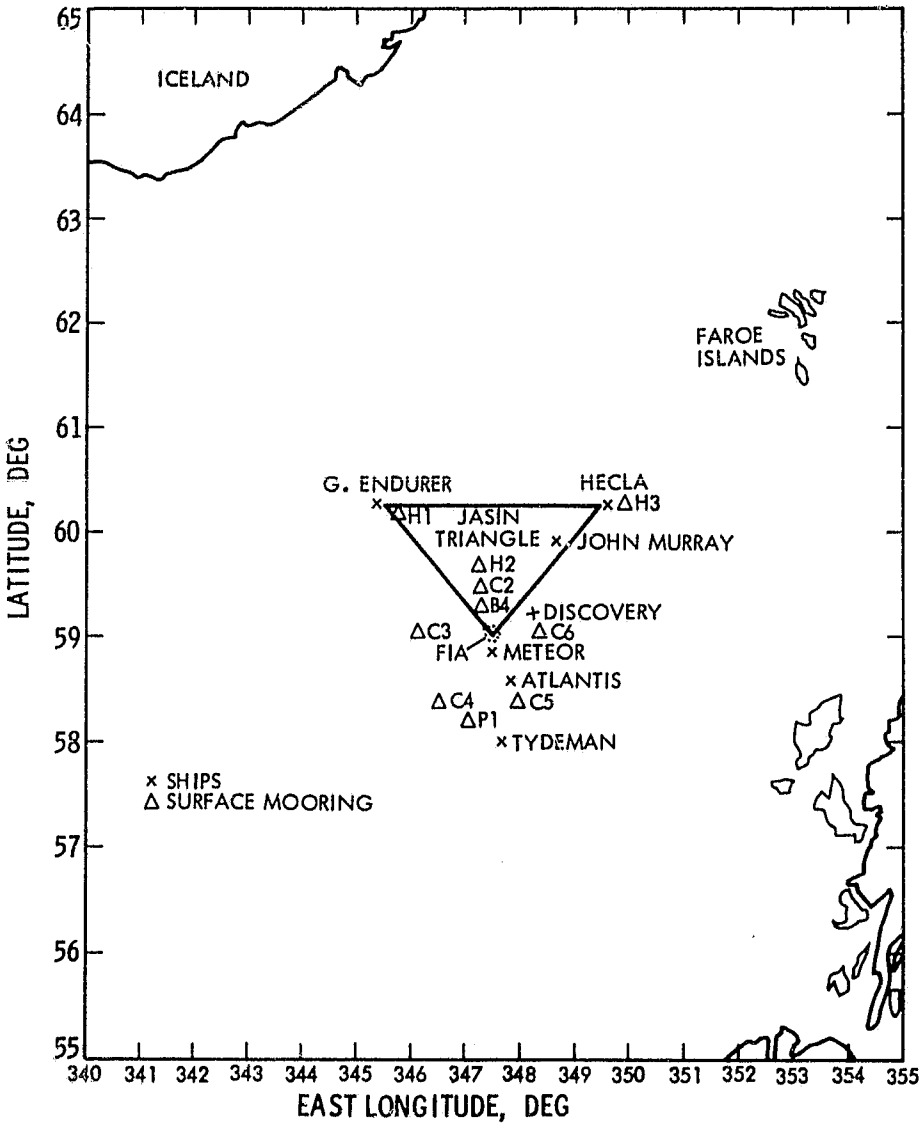

Figure 1. The JASIN experiment platform distribution. Triangles indicate buoys, and crosses indicate ship measurements. Endurer, Hecla, Murray and Meteor are primarily meteorological measurements ships [Brown et al. 1982]

temperature and dry-and wet-bulb temperatures along with the anemometer heights for its inputs. This corrected wind speed for surface stability was used for comparison with SMMR-derived wind speed.

6.3 SMMR wind speed versus surface wind speed

Software was developed to search for satellite observations corresponding to the in situ surface measurements of wind speed. Coincidence was determined from the criteria that satellite observations be within ±0.5 degree latitude and longitude and ±30 minute of surface observations. A set of 134 data was obtained for a range of 3-16 m/sec wind speed. The Seasat SMMR preprocessed data on grid 2 was used to calculate wind speed using different regression equations of each subset (Table 2). The results are given in Table 4. The retrieval accuracy using subsets of two to five SMMR channels are within ±10 per cent with 1.5 m/sec r.m.s. error for two channel retrieval. An example of the scatter plot of SMMR wind speed versus surface wind speed is given in Figure 2. The bias was found to vary from -.09 to -.23 m/sec which is negligibly small. Chester's algorithm gave an rms error of ~2.3 m/sec with a bias of -0.41 m/sec.

7.0 Grid point interpolation of satellite-derived wind fields for map production

In our approach of generating global maps of wind speed, the brightness temperature data were used to obtain wind speed using a linear 2 and 3-channel algorithm. The subsets [10H, 18V], [10H, 18H] and [10V, 18V, 21H] were used for calculating wind speed as these subsets were found to give minimum rms error (Table 4). An average of these three retrieved wind speed was used for further analysis. This method may smooth out the noise in the WS retrieval which may be present as a noisy measurement. WS was thus calculated using data obtained from both ascending and descending revolutions for a given time period. After

Table 4. Results of comparison of wind speed derived from different subsets against in situ neutral density wind speed in JASIN area [59°N, 12.5°W]. 134 data points were used in the comparison and wind speed varied from ∿3-16 m/sec.

Subsets	RMS m/sec	Bias m/sec
10H, 18V	1.46	-0.16
10H, 18H	1.50	-0.23
10V, 10H, 18V	1.62	-0.09
10V, 18V, 21H	1.59	-0.10
10V, 18V, 18H	1.63	-0.12
10V, 10H, 18V, 21V	1.71	-0.13
10V, 10H, 18V, 37V	1.62	-0.12
10V, 10H, 18V, 21H	1.72	-0.12
10V, 10H, 18V, 21H, 37H	1.73	-0.13
Chester's algorithm	2.29	-0.41

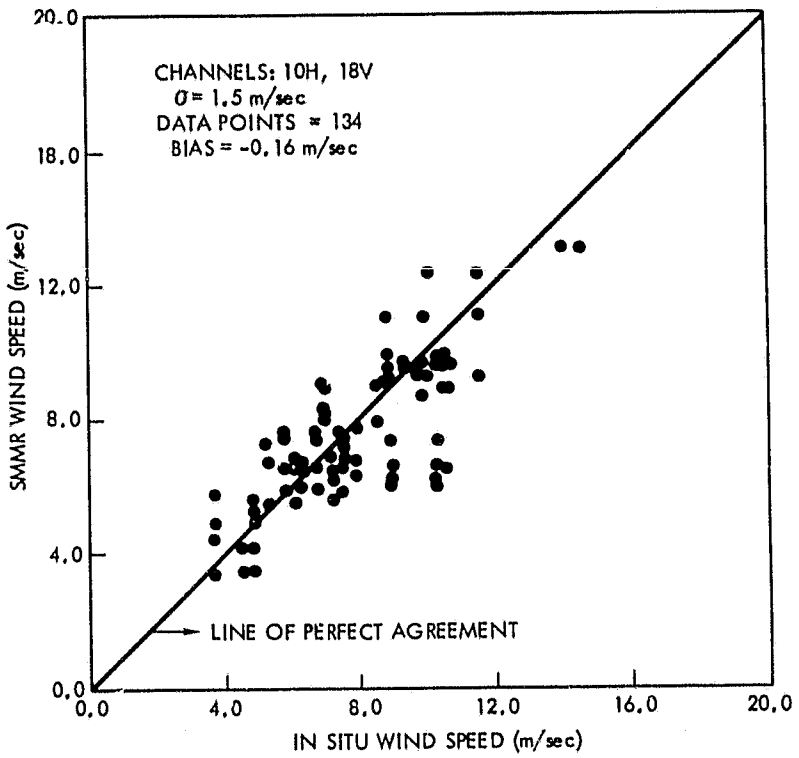

Figure 2. SMMR wind speed comparisons with JASIN surface measurements

filtering the data contaminated with rain, sun glitter, and land, a regular grid of 2°x2° latitude and longitude was filled with interpolated values of the parameter (WS). Each grid point is considered individually with the value assigned at that point determined by a weighted average of all those given data points which lie within some specified distance (2°) of the grid point. This distance is termed as the radius of consideration (ROC) or influence. Therefore, if there are to be a total of N interpolation grid points, then the values of the interpolated parameter P_k is given by

$$P_k = \frac{\sum_{j=1}^{M} W_{jk} P_j}{\sum_{j=1}^{M} W_{jk}} ; \quad k = 1, 2, - - - N$$

where M is the number of given data values P_j within the ROC about the grid point k, and W_{jk} are the weighting factors. The denominator in the above equation is given by the Cressman formula

$$W_{jk} = \frac{D^2 - d_{jk}^2}{D^2 + d_{jk}^2} \quad \leq D$$

$$= 0 \qquad\qquad > D$$

where D is ROC which is 2° and d_{jk} is the distance of data points j from a grid position k.

The regular grid of WS created by this procedure was used as input for the contour program. The software used to generate these contour plots was developed by Chelton at Jet Propulsion Laboratory and implemented on a digital VAX 11/780 using the Pilot Ocean Data System (PODS). To minimize the effect of uneven swath coverage by the satellite, Chelton's software provided a 'box filtering' capability to smooth the data. A 6° longitude by 2° latitude box

filter was used in the analysis. This method of smoothing avoided small scale variations of the wind speed but preserved large scale climatological features.

8. Discussion and intercomparison of SMMR-WS, SASS-WS and ALT-WS global maps

Figures 3 and 4 display the global mean wind speed derived from the SMMR data for the period July 6 to August 7, and July 6 to October 10, 1982, respectively. Several features which conform to the prevailing ideas can be noticed from the map. Roughly between latitudes 30°N and 30°S, the region of tropical easterlies (trades) separated by doldrums (region of light, calm winds) can be seen from the map. These tropical easterlies which originate at low latitude equatorwards of the subtropical high-pressure cells are seen to have remarkable constancy of wind speed. The region of doldrums appears in the eastern and western part of the central Pacific and in the Atlantic it appears towards the eastern part extending to the coast of Brazil. In addition, a small region of doldrums is also evident in the Indian ocean.

Between the region 30°-60° in both hemispheres, the winds are prevailing westerlies, which originate on the poleward side of sub-tropical high. The southern westerlies are stronger than those of northern hemisphere because the broad expanses of ocean prevent the development of stationary pressure systems and hence westerlies - "roaring forties" - there can blow unhindered over the southern ocean around Antarctica. In the northern hemisphere, the path of westerlies is frequently affected by cells of low and high pressure which travel generally eastward within the basic flow. Another region of light and calm winds known as the horse latitudes, separating the tropical easterlies from the stormy westerlies, is also seen in the map. The highest wind speeds are in the southern hemisphere extending from 50°S to Antarctica.

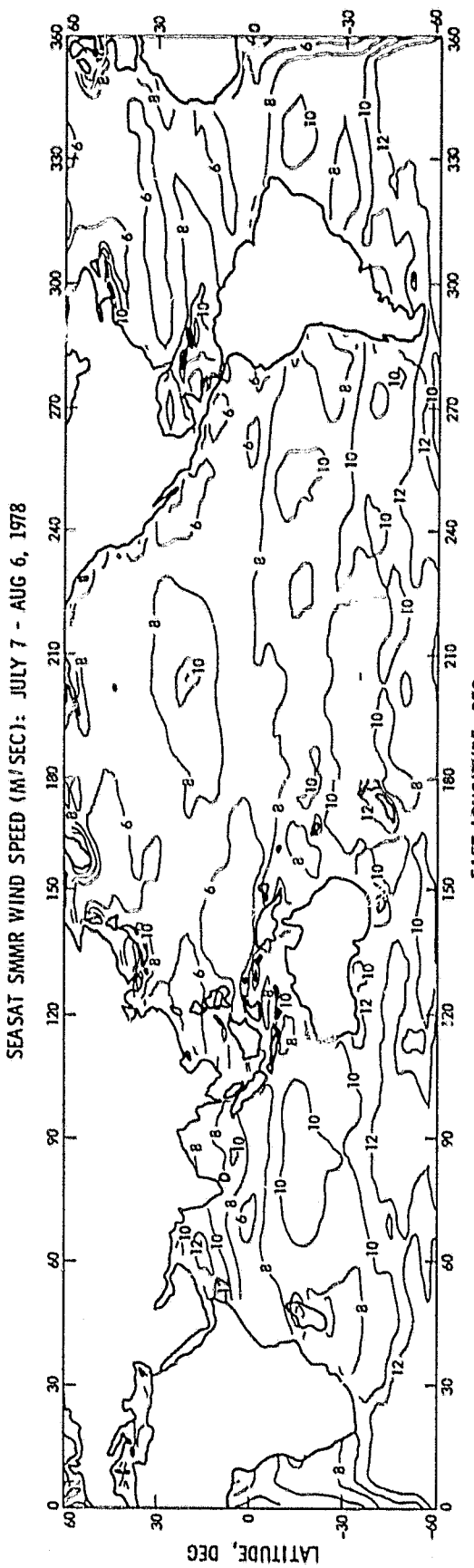

Figure 3. Global distribution of Seasat SMMR wind speed for the period July 7 - August 6, 1978

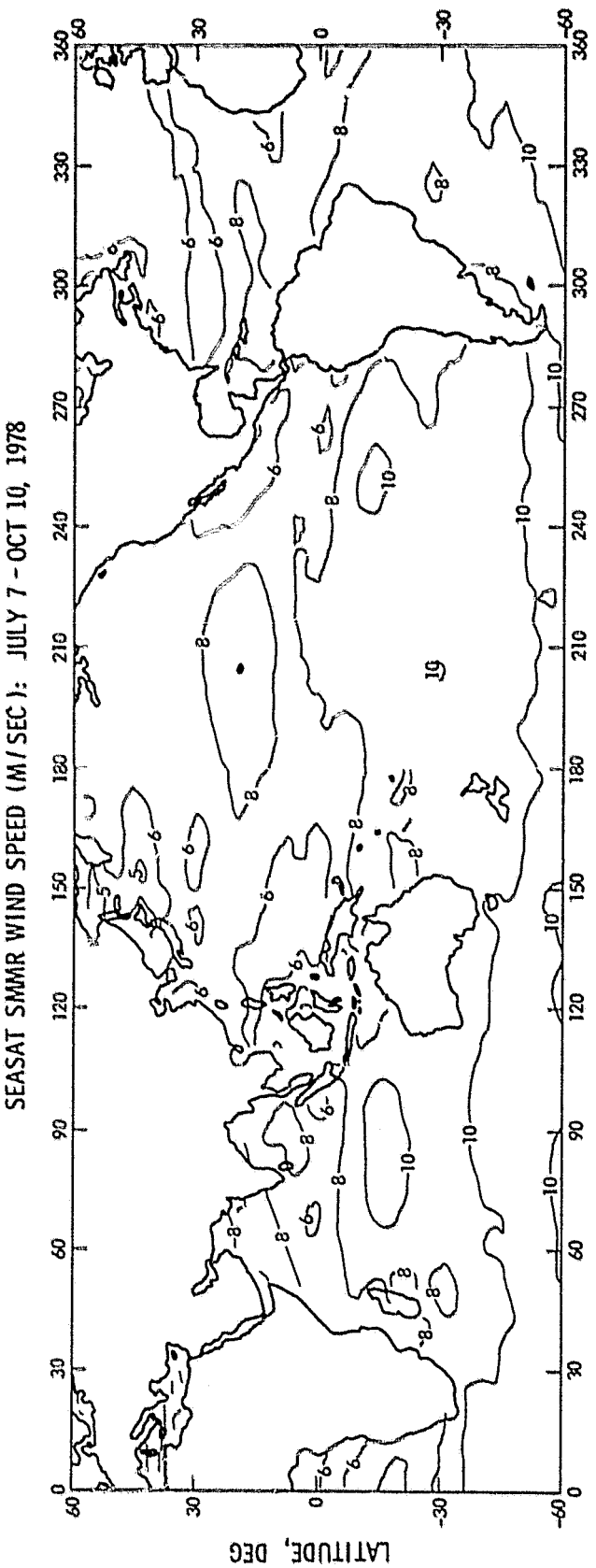

Figure 4. Global distribution of Seasat SMMR wind speed for the period July 7 - Oct. 10, 1978

The characteristics of the wind speed global maps obtained from the three sensors SASS, ALT and SMMR and displayed in Figures 4, 5 and 6 are described below. In the Pacific, the SMMR and the SASS winds show reasonable agreement in magnitude and are slightly higher than the ALT wind speed. In the Indian ocean and in the longitude belt of 0-120°East, the SMMR and the ALT wind fields show reasonable agreement and are lower than that of SASS wind field. The SASS wind field reaches a maximum of ~16 m/sec. In the Atlantic again, SMMR and ALT winds are in reasonable agreement. The SASS winds are generally higher in the southern part of the Atlantic ocean. Figure 6 shows a belt of 6 m/sec wind speed near the coast of California. However, notice that these features are not well pronounced in SMMR and SASS maps (Figures 4 and 5). Some previously unknown features have also been noted by Chelton et al. [1981].

The reason for these discrepancies might be attributed partly to the different field-of-view (FOV) characteristics of the three sensors SMMR, SASS and ALT. The wind field distribution within a FOV may provide different averages if its distribution is inhomogeneous. This is quite likely for wind speed which is highly variable in space and time. Another reason for discrepancies may be the different physical processes responsible for providing their signatures for active (SASS, ALT) and passive (SMMR) sensors. The active sensors measure microwave backscattered power from the surface due to specular reflection and Bragg resonance scattering. The SMMR responds to the emissivity changes. These physical processes of emission and backscattering are closely related to the wind speed. Intercomparisons of wind fields obtained from SMMR, SASS and ALT are being studied in greater detail at Jet Propulsion Laboratory.

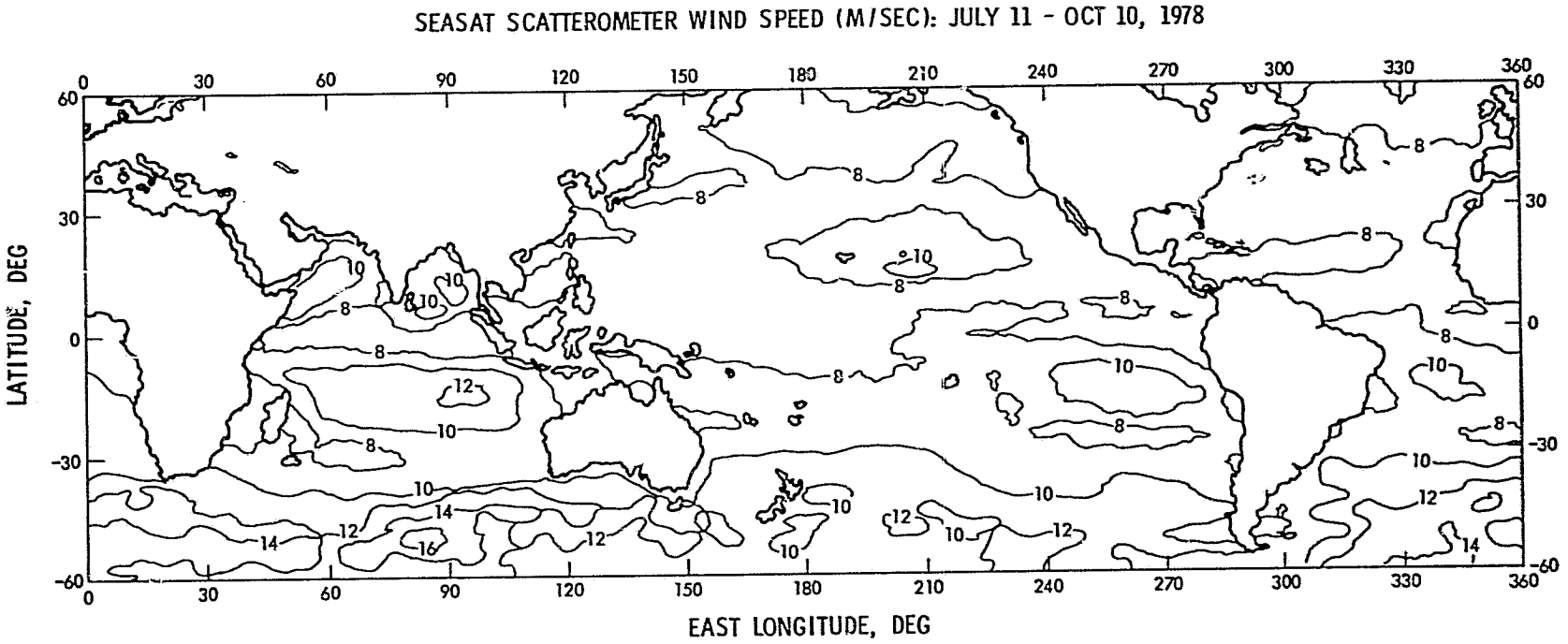

Figure 5. Global distribution of Seasat-A Scatterometer (SASS) wind speed for the period July 11 - Oct. 10, 1978

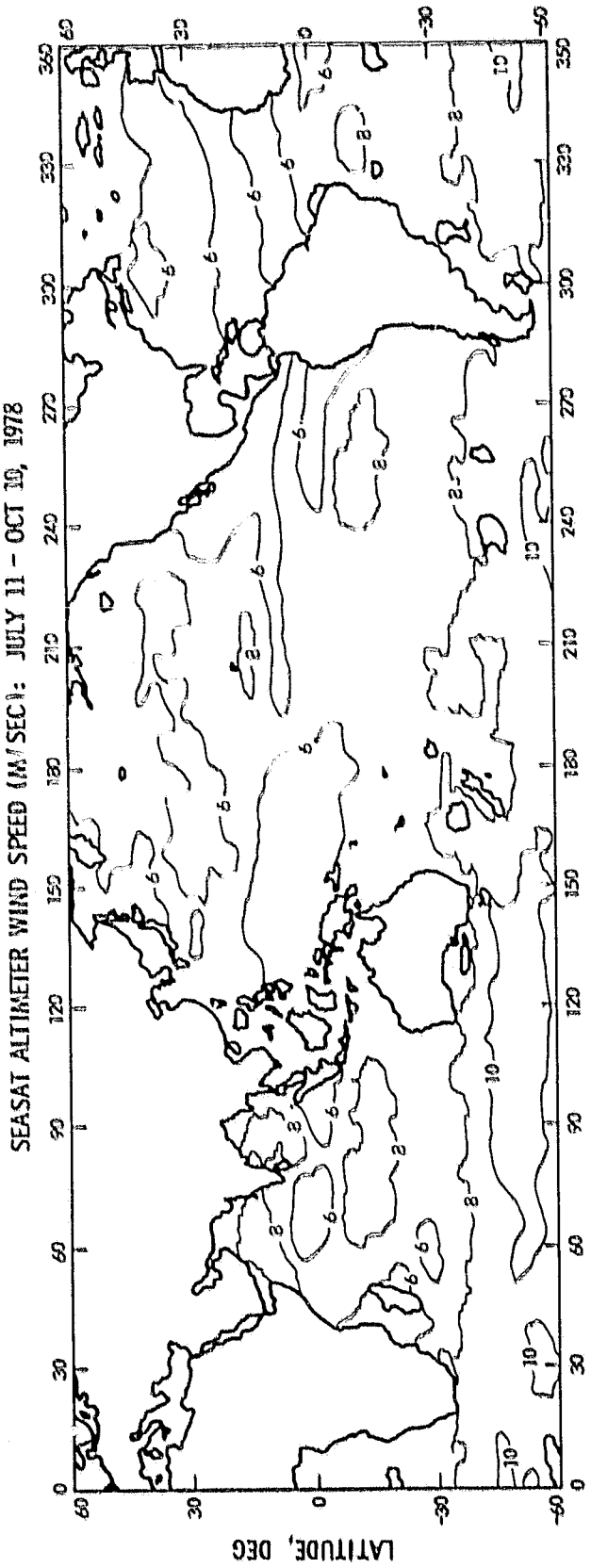

Figure 6. Global distribution of Seasat altimeter (ALT) wind speed for the period July 11 - Oct. 10, 1978

9.0 Conclusions and remarks

The analysis presented in this report demonstrates the usefulness of two and three channels retrievals for wind speed. For the limited in situ observations it appears that the SMMR is capable of providing wind speed to an accuracy of ~1.5 m/sec, comparable to in situ mesurements. However, unless more comparisons at different geographical locations and under varied atmospheric conditions are carried out, it is difficult to conclude the ultimate retrieval accuracy of wind speed from SMMR data and also the optimum subset of SMMR channels for wind speed retrieval.

The global maps of wind speed generated using the present algorithm show the arrangement of averaged winds in well ordered belts. The tropical easterlies are of comparable strength in both hemispheres, but the southern westerlies are stronger than those of northern hemisphere. These satellite derived global maps reveal the features which conform to the prevailing known features. Timely availability of these global maps can enhance our weather forecasting skill considerably in the future and may provide more insight into air-sea interaction studies.

Acknowledgements

The author, an NRC-NASA Senior Resident Research Associate, on leave from Space Applications Center (ISRO), Ahmedabad, India, gratefully acknowledges the support of J. W. Waters, E. G. Njoku, D. Chelton and R. K. Kakar, who reviewed the manuscript and made valuable suggestions; W. T. Liu, who provided the JASIN data, made available his software for the surface layer model and provided many useful comments on the manuscript; D. Chelton, who provided SASS and ALT gridded data for the entire Seasat mission, from which global maps (SASS and ALT) were produced; Stacy Kniffen, who provided software support; Indu Patel, who helped with the software implementation on the VAX-11/780 computer system, and Bonnie S. Beckner, who typed the manuscript. The author thanks the National Research Council for supporting this work at the Jet Propulsion Laboratory.

References

Alishouse, J.C., 1982: Total precipitable water and rainfall determinations from the Seasat Scanning Multichannel Microwave Radiometer (SMMR), NOAA Technical Report NESS 90, National Oceanic and Atmospheric Administration, Washington, D.C.

Bussinger, J.A., R. H. Stewart, T. Guymer, D. B. Lame and G. H. Born, eds., 1980: Seasat-JASIN Workshop report, volume I, Findings and conclusions, JPL publication 80-62, Jet Propulsion Laboratory, Pasadena, CA 91109

Bernstein, R.L., Edr; 1982, Seasat special issue I: Geophysical evaluation, reprinted from J.G.R. vol. 87

Brown, R.A., V.J. Cardone, T. Guymer, J. Hawkins, J.E. Overland, W.J. Pierson, S. Peteherych, J.C. Wilkerson, P.M. Woiceshyn and M. Wurtule, 1982: Surface wind analyses for Seasat, J.G.R., vol 87, pp 3355-3364

Chelton, D. B., K. J. Hussey and M. E. Parke, 1981: Global satellite measurements of water vapor, wind speed and wave height, Nature vol. 294, pp 529-532

Furnival, G.M. and R. W. Wilson, Jr., 1974: Regressions by leaps and bounds, Technometrics, vol. 16, pp 499-511

Grody, N.C., 1976: Remote sensing of atmospheric water content from satellites using microwave radiometry. IEEE Trans. Antennas Propagat., vol AP-24, pp 155-162

Gower, J.F.R., Eds. 1981: The potential impact of scatterometry on oceanography: A wave forecasting case, M.A. Cane and V.J. Cardone, in Oceanography from Space, pp. 587

Hofer, R. and E. G. Njoku, 1981: Regression techniques for oceanographic parameter retrieval using space-borne microwave radiometry, IEEE Trans. on Geoscience and Remote Sensing vol GE-19, pp 178-189.

Liu, W.T., K. B. Katsaros and J.A. Businger, 1979: Bulk parameterization of air-sea exchanges of heat and water vapor including the molecular constraints at the interface, J. Atm. Sci. vol 36, pp 1722-1735

Liu, W.T., and W.G. Large, 1981: Determination of surface stress by Seasat-SASS: A case study with JASIN data, J. Phys. Oceanography, vol. 11, pp 1603-1611

Lipes, R.G., and G.H. Born, 1981: SMMR Mini-Workshop IV, JPL Publication 622-234, Jet Propulsion Laboratory, Pasadena, CA 91109 (an internal document).

Njoku, E.G., 1982: Passive microwave remote sensing of the earth from space - A review, Proc. IEEE, vol 70, pp 728-750

Njoku, E.G., J.M. Stacey and F.T. Barath, 1980: The seasat scanning multichannel microwave radiometer (SMMR): Instrument description and performance, IEEE J. Oceanic Eng. vol OE-5, pp 100-115

Pandey, P.C. and R.K. Kakar, 1983: A two-step linear statistical technique using leaps and bounds procedure for retrieving geophysical parameters from microwave radiometric data, IEEE Trans. Geoscience and Remote Sensing (in press)

Pandey, P.C. and R.K. Kakar 1982: An empirical microwave emissivity model for a foam covered sea, IEEE J. of Oceanic Eng. vol OE-7, pp 135-140

Pandey, P.C. and S. Kniffen, 1982: Evaluation of the potential of one to three Seasat-SMMR channels in retrieving sea surface temperature, JPL publication 82-89, Jet Propulsion Laboratory, California Institute of Technology, Pasadena, CA.

Pandey, P.C., 1982: Precipitable water: Its linear retrieval using leaps and bounds procedure and its global distribution from Seasat SMMR data, JPL publication 82-96, Jet Propulsion Laboratory, California Institute of Technology, Pasadena, CA

Rosenkranz, P.W., 1978: Inversion of data from diffraction limited multiwavelength remote sensors, 1. linear case, Radio Science, vol 13, pp 1003-1010

Wentz, F.J., 1982: Model function for ocean microwave brightness temperature, J. Geophys. Res. (in press)

Wilheit, T.T. and A.T.C. Chang, 1980: An algorithm for retrieval of ocean surface and atmospheric parameters from the observations of the Scanning Multichannel Microwave Radiometer, Radio Science, vol 15, pp 525-544

Waters, J.W., K.F. Kunzi, R.L. Pettyjohn, R.K.L. Poon, and D.H. Staelin, 1975: Remote sensing of atmospheric temperature profile with Nimbus 5 microwave spectrometer, J. Atm. Sci. vol 32, pp 1953-1969

NASA—JPL—Coml., L.A., Calif.